

Dispersive optical constants and temperature tuned band gap energy of $\text{Ti}_2\text{InGaS}_4$ layered crystals

This article has been downloaded from IOPscience. Please scroll down to see the full text article.

2007 *J. Phys.: Condens. Matter* 19 256210

(<http://iopscience.iop.org/0953-8984/19/25/256210>)

[View the table of contents for this issue](#), or go to the [journal homepage](#) for more

Download details:

IP Address: 129.252.86.83

The article was downloaded on 28/05/2010 at 19:22

Please note that [terms and conditions apply](#).

Dispersive optical constants and temperature tuned band gap energy of $\text{Tl}_2\text{InGaS}_4$ layered crystals

K Goksen, N M Gasanly¹ and H Ozkan

Physics Department, Middle East Technical University, 06531 Ankara, Turkey

E-mail: nizami@metu.edu.tr (N M Gasanly)

Received 22 February 2007, in final form 17 May 2007

Published 5 June 2007

Online at stacks.iop.org/JPhysCM/19/256210

Abstract

The optical properties of $\text{Tl}_2\text{InGaS}_4$ layered single crystals have been studied by means of transmission and reflection measurements in the wavelength range of 400–1100 nm. The analysis of the room temperature absorption data revealed the presence of both optical indirect and direct transitions with band gap energies of 2.35 and 2.54 eV, respectively. Transmission measurements carried out in the temperature range of 10–300 K revealed that the rate of change of the indirect band gap with temperature is $\gamma = -4.70 \times 10^{-4} \text{ eV K}^{-1}$. The absolute zero value of the band gap energy was obtained as $E_{gi}(0) = 2.45 \text{ eV}$. The dispersion of the refractive index is discussed in terms of the Wemple–DiDomenico single-effective-oscillator model. The refractive index dispersion parameters: oscillator energy, dispersion energy, oscillator strength and zero-frequency refractive index were found to be 5.73 eV, 31.46 eV, $11.72 \times 10^{13} \text{ m}^{-2}$ and 2.55, respectively. From x-ray powder diffraction study, the parameters of the monoclinic unit cell were determined.

1. Introduction

The potential application of new semiconducting materials in solid state physics requires their growth and detailed examination of their physical properties. Some ternary layered-chain structured semiconductors like the group III chalcogenides (TlGaS_2 , TlInS_2 , TlGaSe_2 and TlInSe_2) have been explored thoroughly. They have already proved to be important for application in optoelectronic devices [1–7]. The compound $\text{Tl}_2\text{InGaS}_4$ belongs to the layered semiconductors group. This crystal is a structural analogue of TlInS_2 and TlGaS_2 , in which half of the indium (gallium) atoms are replaced by gallium (indium) atoms [1, 2]. The crystal lattice consists of alternating two-dimensional layers arranged parallel to the (001) plane. Interlayer bonding in $\text{Tl}_2\text{InGaS}_4$ is formed between Tl and S atoms while the bonding between In(Ga) and S atoms is of the intralayer type. The projections of the crystal structure on the *ac*- and

¹ Author to whom any correspondence should be addressed.

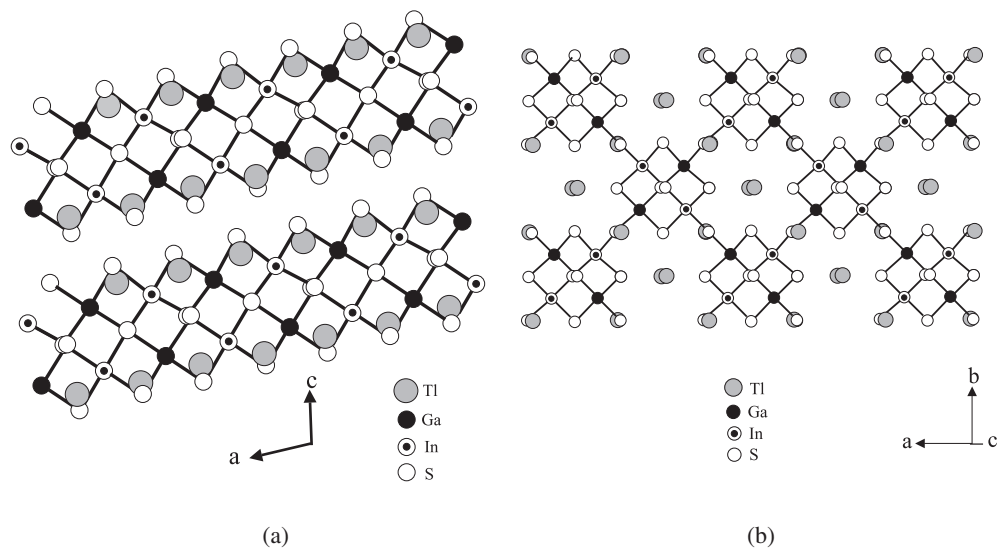


Figure 1. Projection of the crystal structure of $\text{Tl}_2\text{InGaS}_4$ on ac -planes (a) and ab -planes (b), assuming an alternating distribution of Ga and In atoms in the lattice.

ab -planes are presented in figures 1(a) and (b), respectively. The fundamental structural unit of a layer is the $\text{In}_4(\text{Ga}_4)\text{S}_{10}$ polyhedron representing a combination of four elementary tetrahedra $\text{In}(\text{Ga})\text{S}_4$ linked together by bridging S atoms. The thallium atoms are located in trigonal prismatic voids resulting from the combination of the $\text{In}_4(\text{Ga}_4)\text{S}_{10}$ polyhedra into a layer.

Optical and photoelectrical properties of TlInS_2 and TlGaS_2 crystals were studied in [3–7]. The fundamental absorption edges are formed by indirect and direct transitions with $E_{gi} = 2.28$ eV and $E_{gd} = 2.33$ eV (TlInS_2) and $E_{gi} = 2.38$ eV and $E_{gd} = 2.53$ eV (TlGaS_2) [3]. A high photosensitivity in the visible range of spectra and high birefringence in conjunction with a wide transparency range of 0.5 – 14 μm make these crystals useful for optoelectronic applications [7]. Previously, we studied the temperature-dependent photoluminescence spectra of the $\text{Tl}_2\text{InGaS}_4$ crystals in the range of 10 – 150 K and revealed three emission band energies of 1.754 , 2.041 and 2.286 eV [8]. Recently, thermally stimulated current measurements on this layered crystal were carried out. Two shallow trapping centres with activation energies of 4 and 10 meV were detected at low temperatures [9].

The aim of this work is to study the optical properties of $\text{Tl}_2\text{InGaS}_4$ crystal in the wavelength range of 400 – 1100 nm. The room temperature reflectance and transmittance data for this crystal are analysed to identify the refractive index, oscillator energy and strength, dispersion energy, zero-frequency dielectric constant and refractive index. The determination of these optical constants will increase the available physical information. The rate of change of the indirect band gap with temperature is estimated from the temperature dependence of transmission spectra in 10 – 300 K range. Furthermore, the lattice parameters of $\text{Tl}_2\text{InGaS}_4$ crystals are determined from x-ray analysis in the 10° – 75° Bragg angle (2θ) range.

2. Experimental details

Single crystals of $\text{Tl}_2\text{InGaS}_4$ were grown by the Bridgman method from a stoichiometric melt of starting materials. The resulting ingots (yellow-green in colour) showed good optical

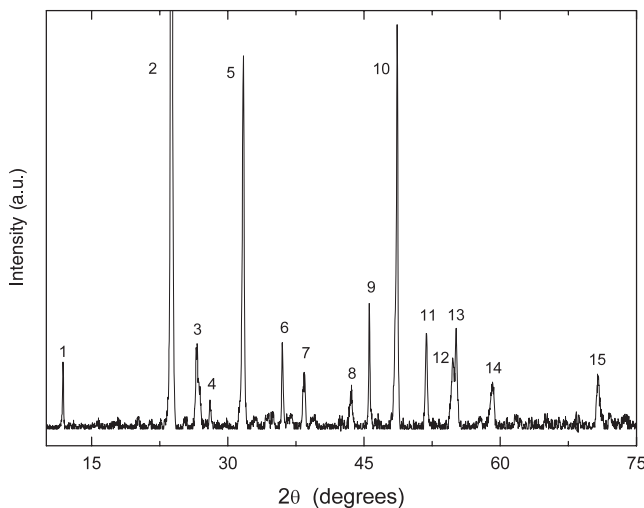


Figure 2. X-ray diffraction pattern of a $\text{Tl}_2\text{InGaS}_4$ powder sample.

quality, and freshly cleaved surfaces were mirror-like. The chemical composition of $\text{Tl}_2\text{InGaS}_4$ crystals was determined by energy dispersive spectroscopic analysis (EDSA) using a JSM-6400 electron microscope. The composition of the studied samples (Tl:In:Ga:S) was found to be 25.9:13.0:13.1:48.0, respectively. Moreover, EDSA indicates that carbon, oxygen and silicon impurities are present in $\text{Tl}_2\text{InGaS}_4$ crystals. The fractional amounts of the impurities were estimated to be somewhat less than 0.1–0.2%.

For the x-ray powder diffraction experiments, a ‘Rigaku Miniflex’ diffractometer with Cu $\text{K}\alpha$ radiation ($\lambda = 0.154\,049$ nm) was used at a scanning speed of $0.02^\circ \text{ s}^{-1}$. Transmission and reflection measurements were carried out with a ‘Shimadzu’ UV-1201 model spectrophotometer by using a 20 W halogen lamp, a holographic grating and a silicon photodiode in the 400–1100 nm wavelength region. For room temperature reflection experiments we utilized the specular reflectance measurement attachment with a 5° incident angle. The resolution of the spectrophotometer was 5 nm. An Advanced Research Systems model CSW-202 closed-cycle helium cryostat was used to cool the sample from room temperature down to 10 K, and the temperature was controlled within an accuracy of ± 0.5 K.

3. Results and discussion

Figure 2 presents the x-ray diffractogram of $\text{Tl}_2\text{InGaS}_4$ crystal (Cu $\text{K}\alpha$). The Miller indices (hkl), the observed and calculated interplanar spacings (d) and the relative intensities (I/I_0) of the diffraction lines are listed in table 1. The lattice parameters of the monoclinic unit cell, recalculated by using a least-squares computer program, DICVOL 04, were found to be $a = 0.9133(3)$, $b = 0.3603(1)$, $c = 1.1604(4)$ nm and $\beta = 95.20^\circ$. Small amounts of the detected impurities are expected to reside at the interstitial positions. We assume that they do not change the calculated lattice parameters within our cited accuracy.

For $\text{Tl}_2\text{InGaS}_4$ single crystals, the transmittance (T) and reflectivity (R) spectra were recorded in the 400–1100 nm wavelength (λ) range (figure 3). The reflectivity of the material with refractive index n and absorption coefficient α is given by [10]

$$R = \frac{(n-1)^2 + (\frac{\alpha\lambda}{4\pi})^2}{(n+1)^2 + (\frac{\alpha\lambda}{4\pi})^2}. \quad (1)$$

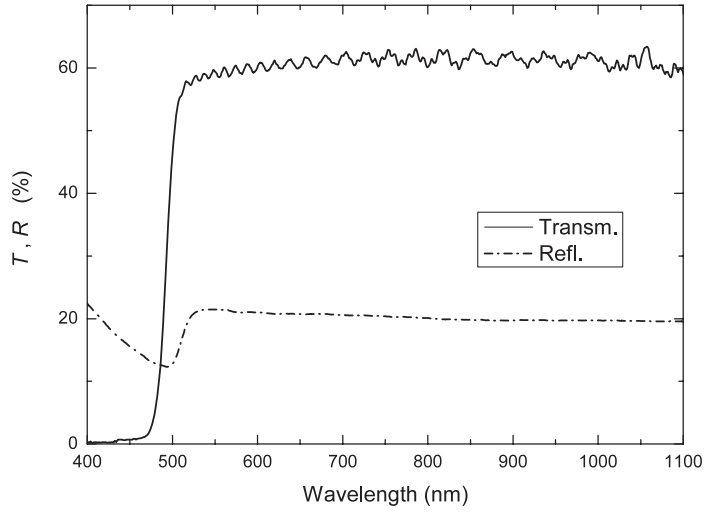


Figure 3. The spectral dependence of transmittance and reflectivity for $\text{Tl}_2\text{InGaS}_4$ crystal at $T = 300$ K.

Table 1. X-ray powder diffraction data for $\text{Tl}_2\text{InGaS}_4$ crystals.

No.	h	k	l	d_{obs} (nm)	d_{calc} (nm)	I/I_0
1	1	0	-1	0.7468	0.7460	3
2	2	0	-2	0.3735	0.3736	100
3	0	1	1	0.3346	0.3345	4
4	1	1	1	0.3182	0.3185	2
5	0	1	2	0.2820	0.2821	15
6	3	0	-3	0.2493	0.2492	4
7	3	1	-2	0.2338	0.2339	2
8	4	1	-2	0.2078	0.2077	2
9	5	0	2	0.1989	0.1987	5
10	4	0	-4	0.1870	0.1870	16
11	5	0	3	0.1762	0.1761	4
12	0	2	2	0.1674	0.1674	3
13	1	2	-2	0.1664	0.1664	4
14	6	0	3	0.1561	0.1562	2
15	2	1	6	0.1332	0.1332	2

The transmittance is represented by the expression [10]

$$T = \frac{(1 - R)^2 \exp(-\alpha d)}{1 - R^2 \exp(-2\alpha d)}, \quad (2)$$

where d is the sample thickness. By using these relations, n and α can be determined from the measurements of reflectivity and transmittance.

The reflectivity is measured using specimens with natural cleavage planes and a thickness such that $\alpha d \gg 1$. The sample is then reduced in thickness (by repeated cleaving using transparent adhesive tape) until it is convenient for transmission measurements. The thickness is determined using transmission interference fringes at a wavelength slightly longer than the intrinsic absorption edge, i.e. in a region with relatively high transmission (figure 3). For this purpose, the long wavelength value of the refractive index $n = 2.60$ obtained from the

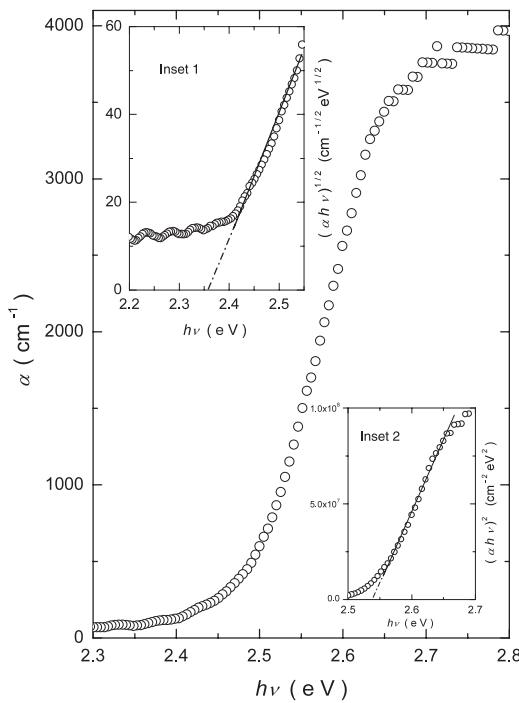


Figure 4. The variation of absorption coefficient as a function of photon energy at $T = 300$ K. Insets 1 and 2 represent the dependences of $(\alpha h\nu)^{1/2}$ and $(\alpha h\nu)^2$, respectively, on photon energy.

reflection measurements was used. In most cases the sample thickness was about $10\ \mu\text{m}$ for room temperature transmission measurements.

The dependence of the absorption coefficient on photon energy is analysed in the high absorption regions to obtain detailed information about the energy band gaps. The absorption coefficient α and photon energy can be related by [10]

$$(\alpha h\nu) = A(h\nu - E_g)^p. \quad (3)$$

In this equation, A is a constant that depends on the transition probability and p is an index that characterizes the optical absorption process, and it is theoretically equal to 2 and $1/2$ for indirect and direct allowed transitions, respectively.

Figure 4 shows the calculated room temperature absorption coefficient α for $\text{Tl}_2\text{InGaS}_4$ crystal in the photon energy range $2.30\text{--}2.70\ \text{eV}$. It was found that α changes from 70 to $3800\ \text{cm}^{-1}$ with increasing photon energy from 2.30 to $2.70\ \text{eV}$. Analysis of the experimental data shows that the absorption coefficient is proportional to $(h\nu - E_g)^p$ with $p = 2$ and $1/2$ for the ranges $2.20\text{--}2.54$ and $2.56\text{--}2.70\ \text{eV}$, respectively. Insets 1 and 2 of figure 4 display the dependences of $(\alpha h\nu)^{1/2}$ and $(\alpha h\nu)^2$ on photon energy $h\nu$, respectively. The circles are the experimental data that were fitted to a linear equation (the solid lines) for finding the band gaps. Linear dependences were observed for the relations $(\alpha h\nu)^{1/2}$ and $(\alpha h\nu)^2$ versus $h\nu$. This suggests the realization of indirect and direct allowed transitions for $\text{Tl}_2\text{InGaS}_4$ crystal over the ranges $2.20\text{--}2.54$ and $2.56\text{--}2.70\ \text{eV}$, respectively. The extrapolations of the straight lines down to $(\alpha h\nu)^{1/2} = 0$ and $(\alpha h\nu)^2 = 0$ give the values of indirect and direct band gap energies $E_{gi} = 2.35 \pm 0.02$ and $E_{gd} = 2.54 \pm 0.02\ \text{eV}$, respectively.

Figure 5 shows the transmission spectra for $\text{Tl}_2\text{InGaS}_4$ crystal registered in the temperature range of $10\text{--}300\ \text{K}$. Since the thin layered samples were very fragile, they broke into pieces at

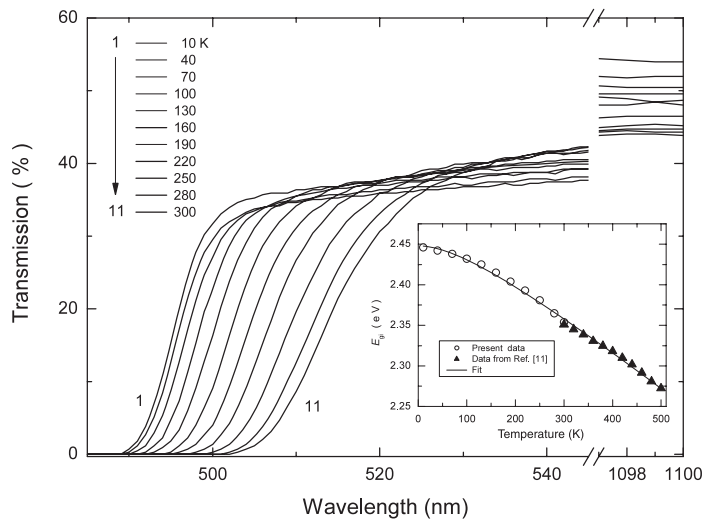


Figure 5. The spectral dependence of transmittance for $\text{Tl}_2\text{InGaS}_4$ crystal in the temperature range 10–300 K. Inset: the indirect band gap energy as a function of temperature. The solid line represents the fit using equation (4).

low temperatures. Therefore, the low-temperature measurements were made on thick samples (about 200 μm). As a consequence, we were able to analyse the temperature dependence of the indirect energy band gap (E_{gi}) only. For technical reasons we were unable to measure the reflection at low temperatures directly. Therefore, for the calculation of the absorption coefficient α , the spectral dependence of room temperature reflectivity was uniformly shifted in energy according to the blue shift of the absorption edge.

The obtained value of the indirect transition energy gap decreases with increasing temperature, as illustrated in the inset of figure 6. Namely, it shifts from 2.45 to 2.35 eV as the temperature increases from 10 to 300 K. The experimental data for the indirect energy band gap of $\text{Tl}_2\text{InGaS}_4$ crystal in the high temperature range of 300–500 K were taken from [11]. The temperature dependence of the energy band gap can be represented by the relation [10]

$$E_{\text{gi}}(T) = E_{\text{gi}}(0) + \frac{\gamma T^2}{T + \beta}. \quad (4)$$

Here, $E_{\text{gi}}(0)$ is the absolute zero value of the band gap, $\gamma = \text{d}E_{\text{gi}}/\text{d}T$ is the rate of change of the band gap with temperature and β is approximately the Debye temperature. The data for the $E_{\text{gi}}-T$ dependence (inset of figure 5) were fitted using equation (4). The fitting of equation (4) is represented by the solid line in the figure, revealing the fitting parameters as $E_{\text{gi}}(0) = 2.45$ eV, $\gamma = -4.70 \times 10^{-4}$ eV K $^{-1}$ and $\beta = 169$ K. It should be noted that the Debye temperature for $\text{Tl}_2\text{InGaS}_4$ crystal was found to be $\beta = 173$ K, estimated by Lindemann's melting rule [12] using x-ray results reported in the first paragraph and a melting temperature $T_m = 1103$ K.

The refractive index n as a function of wavelength, calculated using equations (1) and (2), is shown in figure 6. As seen from this figure, the refractive index in the energy region of $h\nu < E_g$ gradually decreases from 2.72 to 2.60 with increasing wavelength in the range 543–1100 nm. The long wavelength value of refractive index is consistent with the values 2.7 ($\lambda = 800$ nm) and 2.6 ($\lambda = 1100$ nm) reported for TlInS_2 [13] and TlGaS_2 [14] single crystals, respectively.

The dispersive refractive index data in $h\nu < E_g$ range were analysed according to the single-effective-oscillator model proposed by Wemple and DiDomenico [15, 16], which was

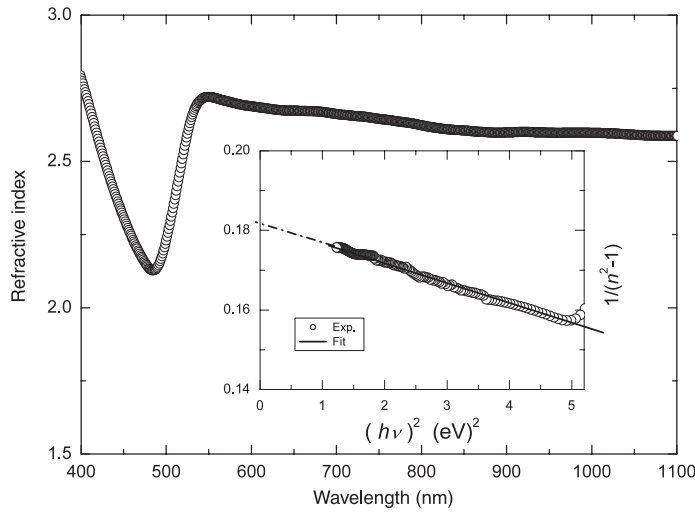


Figure 6. The dependence of refractive index on the wavelength for $\text{Tl}_2\text{InGaS}_4$ crystal. Inset: plot of $(n^2 - 1)^{-1}$ versus $(h\nu)^2$. The solid line represents the fit using equation (5).

successfully applied to the experimental data for the ternary TlGaSe_2 and TlGaS_2 layered crystals [17, 14]. The refractive index is related to photon energy through the relationship

$$n^2(h\nu) = 1 + \frac{E_{\text{so}}E_{\text{d}}}{E_{\text{so}}^2 - (h\nu)^2}, \quad (5)$$

where E_{so} is the single oscillator energy and E_{d} is the dispersion energy. Plotting $(n^2 - 1)^{-1}$ versus $(h\nu)^2$ allows the determination of the oscillator parameters by fitting a linear function to the lower energy data range (1.13–2.25 eV). The fitting of the above reported function is presented in the inset of figure 6. The zero-frequency dielectric constant $\varepsilon_0 = n_0^2 = 6.49$ and refractive index $n_0 = 2.55$ were evaluated by means of equation (5). The oscillator energy E_{so} is an ‘average’ energy gap and, to a fair approximation, it is associated empirically with the lowest direct band gap E_{gd} by the relationship $E_{\text{so}} \approx 2.0 E_{\text{gd}}$ [18–21]. The ratio $E_{\text{so}}/E_{\text{gd}}$ for $\text{Tl}_2\text{InGaS}_4$ crystal, determined in this study, was found to be 2.25.

The values of the parameters E_{so} and E_{d} were calculated from the slope and the intersection with the y -axis of the straight line (inset of figure 6) as 5.73 and 31.46 eV, respectively. Moreover, the values of the zero-frequency dielectric constant $\varepsilon_0 = n_0^2 = 6.49$ and refractive index $n_0 = 2.55$ were evaluated by means of equation (5). The oscillator energy E_{so} is an ‘average’ energy gap and, to a fair approximation, it is associated empirically with the lowest direct band gap E_{gd} by the relationship $E_{\text{so}} \approx 2.0 E_{\text{gd}}$ [18–21]. The ratio $E_{\text{so}}/E_{\text{gd}}$ for $\text{Tl}_2\text{InGaS}_4$ crystal, determined in this study, was found to be 2.25.

The refractive index n can also be analysed to determine the oscillator strength S_{so} for $\text{Tl}_2\text{InGaS}_4$ crystal. The refractive index is represented by a single Sellmeier oscillator at low energies [22]

$$\frac{(n_0^2 - 1)}{(n^2 - 1)} = 1 - \left(\frac{\lambda_{\text{so}}}{\lambda} \right)^2, \quad (6)$$

where λ_{so} is the oscillator wavelength. Rearranging equation (5) gives [19]

$$(n^2 - 1)^{-1} = \frac{1}{S_{\text{so}}\lambda_{\text{so}}^2} - \frac{1}{S_{\text{so}}\lambda^2}. \quad (7)$$

Here, $S_{\text{so}} = (n_0^2 - 1)/\lambda_{\text{so}}^2$. The values of S_{so} and λ_{so} calculated from the $(n^2 - 1)^{-1}$ versus λ^{-2} plot were found to be $11.72 \times 10^{13} \text{ m}^{-2}$ (180.27 eV 2) and $2.16 \times 10^{-7} \text{ m}$, respectively. The

value obtained for the oscillator strength is of the same order as those obtained for ZnS, ZnSe, Ag₂S, GeSe₂ and TlGaS₂ crystals [16, 23, 20, 14].

4. Conclusions

Tl₂InGaS₄ crystals were characterized by x-ray powder diffraction analysis. The parameters of the monoclinic unit cell were found to be $a = 0.9133$, $b = 0.3603$, $c = 1.1604$ nm and $\beta = 95.20^\circ$. The optical transmission and reflection of Tl₂InGaS₄ crystals were measured over the 400 and 1100 nm spectral region in order to derive the absorption coefficient and refractive index. The analysis of the room temperature absorption data revealed the coexistence of indirect and direct transitions in Tl₂InGaS₄ crystals with energy band gaps of 2.35 and 2.54 eV, respectively. The absorption edge was observed to shift toward lower energy values as temperature increases from 10 to 300 K. The data were used to calculate the indirect energy band gap of the crystal as a function of temperature. The rate of change of the indirect band gap with temperature was determined as $\gamma = -4.70 \times 10^{-4}$ eV K⁻¹. The absolute zero value of the band gap energy was found to be $E_{gi}(0) = 2.45$ eV. The refractive index dispersion data were analysed using the Wemple–DiDomenico single-effective-oscillator model. As a result, the oscillator energy, dispersion energy, oscillator strength and zero-frequency refractive index were determined.

References

- [1] Yee K A and Albright A 1991 *J. Am. Chem. Soc.* **113** 6474
- [2] Muller D and Hahn H 1978 *Z. Anorg. Allg. Chem.* **438** 258
- [3] Hanias M, Anagnostopoulos A, Kambas K and Spyridelis J 1989 *Physica B* **160** 154
Hanias M, Anagnostopoulos A, Kambas K and Spyridelis J 1992 *Mater. Res. Bull.* **27** 25
- [4] Samedov S R, Baykan O and Gulubayov A 2004 *Int. J. Infrared Millim. Waves* **25** 735
- [5] Ibragimov T D and Aslanov I I 2002 *Solid State Commun.* **123** 339
- [6] Akhmedov A M, Bakhshov A E, Lebedev A A and Yakobson M A 1978 *Sov. Phys.—Semicond.* **12** 299
- [7] Allakhverdiev K R 1999 *Solid State Commun.* **111** 253
- [8] Goksen K, Gasanly N M and Ozkan H 2005 *J. Korean Phys. Soc.* **47** 267
- [9] Mogaddam N A P, Yuksek N S, Gasanly N M and Ozkan H 2006 *J. Alloys Compounds* **417** 23
- [10] Pankove J I 1971 *Optical Processes in Semiconductors* (Englewood Cliffs, NJ: Prentice-Hall)
- [11] Qasrawi A F and Gasanly N M 2007 *Opt. Mater.* at press
- [12] Drabble J R and Goldsmid H J 1961 *Thermal Conduction in Semiconductors* (Oxford: Pergamon) p 191
- [13] Kalomiros J A and Anagnostopoulos A N 1994 *Phys. Rev. B* **50** 7488
- [14] Qasrawi A F and Gasanly N M 2005 *Phys. Status Solidi a* **202** 2501
- [15] Wemple S H and DiDomenico M 1971 *Phys. Rev. B* **3** 1338
- [16] Wemple S H and DiDomenico M 1969 *Phys. Rev. Lett.* **23** 1156
- [17] El-Nahass M M, Sallam M M, Rahman S A and Ibrahim E M 2006 *Solid State Sci.* **8** 488
- [18] Tanaka K 1980 *Thin Solid Films* **66** 271
- [19] Yakuphanoglu F, Cukurovali A and Yilmaz I 2004 *Physica B* **351** 53
Yakuphanoglu F, Cukurovali A and Yilmaz I 2004 *Physica B* **353** 210
- [20] Marguez E, Nagels P, Gonzalez-Leal J M, Bernal-Oliva A M, Sleenckx E and Callaerts R 1999 *Vacuum* **52** 55
- [21] Marguez E, Bernal-Oliva A M, Gonzalez-Leal J M, Pricto-Alcon R, Ledesma A, Jimenez-Garay R and Martil I 1999 *Mater. Chem. Phys.* **60** 231
- [22] Walton A K and Moss T S 1963 *Proc. Phys. Soc.* **81** 509
- [23] El-Nahass M M, Farag A M, Ibrahim E M and Rahman S A 2004 *Vacuum* **72** 453